Niessink Tom (Orcid ID: 0000-0002-8621-9868)

Otto Cees (Orcid ID: 0000-0001-6955-4843)

Raman hyperspectral imaging detects novel and combinations of crystals in synovial fluids of patients with a swollen joint

Authors: Tom Niessink (MSc.)[1,2*], Charline Kuipers (MSc.)[1], Brighton Z. de Jong (BSc.)[1], Aufried T.M. Lenferink (Bsc.)[1], Matthijs Janssen (MD., PhD.)[2], Tim L Jansen (MD., PhD.)[1,2], and Cees Otto (PhD.)[1]

AFFILIATIONS:

1: Medical Cell BioPhysics group, University of Twente, Drienerlolaan 5, 7500AE, Enschede, the Netherlands

2: Department of Rheumatology, VieCuri Medical center, Tegelseweg 210, 5912 BL, Venlo, the Netherlands

ABSTRACT: The identification of synovial crystals is important for diagnosing rheumatic diseases. Currently, rheumatologists worldwide use compensated polarized light microscopy (CPLM) for crystal identification, but this technique is flawed. Raman spectroscopy might offer an objective, accurate alternative. We have tested Raman hyperspectral imaging on synovial fluid samples of 28 patients with swollen joints, measuring 5-10 crystals in each of these. Reference spectra for identification were measured using patient material, synthetic compounds, and oxalate kidney stones. Additionally, RRUFF and PANGAEA Raman databases were used to identify spectra. We identified the classical pathological crystals monosodium urate for gout and calcium pyrophosphate for calcium pyrophosphate deposition disease (CPPD). Hydroxyapatite, lipid spherules, and calcium oxalate monohydrate have also been observed and had been previously identified in synovial fluids. Other crystals (7), which were not previously observed in synovial fluid using CPLM, have been identified as well: calcite, aragonite, anatase, rutile, thenardite, dolomite, and a carotenoid. In addition, we found combinations of crystals in 13 out of 28 patients. We propose that the observed large variation of detectable crystals from a small population of patients and a small number of crystals per patient has significant ramifications for the use of compensated polarized light microscopy for the diagnosis of gout and CPPD. Further studies are required to learn the clinical significance of these crystals in human arthritis. **Keywords: Raman hyperspectral imaging, diagnostics, gout, calcium pyrophosphate arthritis, rheumatology**

1. Introduction

Deposits of crystals cause many medical disorders, called crystallopathies, that can manifest as either acute or chronic organ injuries[1]. In rheumatology, gout, and calcium pyrophosphate disease (CPPD) are together the most important auto-inflammatory arthritic crystallopathies, with a prevalence between 1-7%[2,3]. There is a large similarity in symptoms between gout and CPPD. This makes it difficult to diagnose these diseases based on symptoms alone, and they are easily mistaken for each other[2,3]. Because the treatment strategies for both diseases are completely different, an accurate method for diagnosis is important[4,5].

The current standard in the diagnosis of gout and CPPD is compensated polarized light microscopy (CPLM)[2,3]. In CPLM, a rheumatologist will examine synovial fluid (SF) aspirates for the

presence of pathologic crystals. The presence of monosodium urate (MSU) negatively birefringent crystals is known as a strong biomarker for gout, while the presence of calcium pyrophosphate (CPP) weak positively birefringent crystals is known as a strong biomarker for CPPD. The rheumatologist will study the morphology, size, and birefringence of the SF crystals.

While rheumatologists are depending on CPLM, it has suboptimal reliability as a diagnostic tool. First reports on the poor reproducibility, sensitivity, and specificity of the modality stem from 1986-1998[6-9]. Some of the surveyed centers had a mere 50% accuracy rate in the diagnosis of crystallopathies. More recent studies showed that the accuracy of detection is heavily dependent on the observer's training and that the current educational methods might be insufficient[10,11]. Most often, a diagnosis of gout is more accurate than CPPD. Berendsen et al.[11] (2017) showed a correct identification of images displaying pathognomonic MSU crystals by 81% and CPP crystals by 68% of participants. Especially less-typical morphology crystals are difficult to identify. This is problematic in diseases that require accurate diagnoses.

Raman spectroscopy is approaching the clinic and can be used to support rheumatology diagnostics[12]. The ability to detect MSU and CPP crystals in SF was already shown in 1991[13]. Curran et al.[14,15] (2015) demonstrated a simple in vivo Raman scanner which could detect MSU crystals in the first metatarsophalangeal (big toe) joints of gout patients. They detected MSU in seven out of ten gout patients and one out of ten patients with osteoarthritis. A more advanced method is demonstrated by Li et al.[16-18]. They built a point-of-care Raman device which they tested on 174 gout and CPPD samples. In 89.7% of the samples, there was a consistency with CPLM. Zhang et al.[19] used Stimulated Raman Scattering (SRS) to study MSU and CPP in synovial fluid of rats and 2 patients. They demonstrated large contrast between MSU, CPP crystals, and the non-Raman-scattering background.

In our experiment, we apply the use of hyperspectral Raman imaging (HRI) to identify synovial crystals in 28 patients with suspected gout or CPPD. We demonstrate that alongside MSU and CPP HRI can identify a whole range of crystals in synovial fluids, including various types of titanium dioxide, calcium carbonate, and sodium sulfate particles. We additionally found that simultaneous presentation of multiple crystal types is much more frequent than previously thought and previously was detectable with CPLM. The clinical meaning of these novelties remains to be determined, but these results demonstrate the importance of an accurate, objective diagnostic method to identify these crystals.

2. Materials and Method

2.1 Samples

For this study, we retrieved 28 synovial fluid aspirates from patients with arthritis suspected of gout or acute CPPD from VieCuri Medisch Centrum in Venlo, the Netherlands. The cohort included patients from both sexes and varying age groups, although all patients were adults over 18. Material was collected anonymously according to local law and biomedical research ethics regulations. Around 180 objects were analyzed. Next to the patient samples, different synthetic crystals were measured to create reference spectra for identification: MSU (InvivoGen), CPP (InvivoGen), Cholesterol powder (Sigma Aldrich), Calcium Oxalate Monohydrate (COM, Sigma Aldrich), Hydroxyapatite (HA, Sigma Aldrich), methylprednisolone acetate (Depo Medrol), and triamcinolone acetonide (Kenacort). Samples were prepared by pipetting a 30-40 µl droplet of sample on a microscope slide. This was covered using a standard cover glass.

2.2 Measurements

The HRI setup was built on an Olympus BX41 upright microscope. This was operated with a 40x 0.95NA super apochromatic objective (Olympus). For crystal identification, two polarizer filters were placed in the light path of the microscope. This allowed us to do polarized light microscopy and detect birefringent objects.

The Raman spectroscope was powered by a 647.09 nm Krypton-ion laser (Innova 70C ion laser, Coherent). Raman scattered light was dispersed in a homebuilt spectrometer and photons were collected with a CCD sensor (Andor Newton DU970P-BVF).

Prior to the measurements, several calibration measurements were performed. The pixel-to-wavenumber conversion was calculated using liquid toluene and argon-mercury lamp measurements. A white light tungsten-halogen lamp measurement was used for intensity correction as the transmission of light in the Raman setup is wavelength-dependent.

For crystal identification, the Raman spectrum was measured from 0-3600 cm^{-1} for each pixel/location on a 40x40 grid in a frame of 10x10 µm. The laser spot size was 400 nm and the laser power was 35 mW. Spectra were accumulated in 250 ms per pixel, which makes a total measurement time of ~7 minutes per scanned area containing a crystal.

2.3 Hierarchical Cluster Analysis

The result of the raster scan is a 3D matrix, with both spatial and spectral information. We applied hierarchical cluster analysis with the MATLAB (R2021a, MathWorks, Natick, MA) function *linkage*, using Euclidian distances as the similarity metric. With the MATLAB function *cluster*, we can plot a defined number of clustering. The spectra from all spectra assigned to the cluster are averaged in a cluster spectrum.

2.4 PCA Crystal identification

For crystal identification, a background-corrected crystal spectrum is convenient. To obtain this from the hyperspectral data set, we applied principal component analysis (PCA). PCA score plots were used to threshold the variance of the crystal and separate the crystal data from the background data. Both sets of spectra, crystalline, and background, were then averaged. The MATLAB function *lsqlin* was subsequently used to correct the crystal spectra for the background spectrum. This is a robust method of separating crystal spectra from background spectra.

We obtained Raman spectra from patient material and synthetic crystals and used these to create a database with reference spectra. Identification of the patients' crystal spectra was performed using Pearson's correlation coefficient. For each spectrum in the database, a correlation between the sample and the reference was calculated. All spectra with a correlation >0.8 were considered to be a match. Correlations >0.6 and possible conflicts (2 or more matches with a correlation coefficient >0.8) were checked manually. If no match could be found, geological Raman crystal databases RRUFF and PANGAEA (Planetary ANalogue Geological and Astrobiological Exercise for Astronauts) were consulted with a similar algorithm[20,21]. If the spectrum could be identified, it was classified as such and added to the database.

3. Results and discussion

3.1 Raman cluster analysis

HRI showed the ability to detect and identify individual crystals in SF. Examples of Raman cluster analysis images of identified crystals are shown in Fig. S1 (Supporting Information).

We identified four known pathological crystals, MSU with the characteristic 630 cm^{-1} peak, CPP with the characteristic 1050 cm^{-1} peak, Calcium Oxalate Monohydrate and Hydroxyapatite.

The presence of MSU is a direct indication for gout, and CPP is a direct indication for CPPD. The ability of Raman Spectroscopy to discriminate between these crystals is demonstrated before. The ability to also identify COM (Oxalate arthritis and hyperoxaluria[22]) and HA (hydroxyapatite deposition disease and Milwaukee shoulder syndrome[23]) is an advantage of our approach over more macroscopic methods (Li et al., Curran et al.) or a non-spectroscopic Raman method as performed by Zhang et al who applied SRS on a single waveband.

In addition to crystals that are known to be pathologically relevant, we also identified seven crystals that were not previously found in SF. These are calcite and aragonite, anatase and rutile, thenardite, dolomite and a carotenoid compound.

Calcite and aragonite are calcium carbonate ($CaCO_3$) polymorphs. Calcite is identified with characteristic peaks at 712 and 1086 cm^{-1} and aragonite with characteristic peaks at 708 and 1085 cm^{-1}, which is a subtle but noticeable difference in the Raman spectrum. Calcium carbonate is a known component of gallstones and small carbonate crystals (<1μm) can be found in pancreatic juice[24]. These crystals are negatively birefringent (Δn = -0.172). In vitro studies have shown that uptake of aragonite can trigger IL-8 and TNF-α cytokine release from THP-1 cells[25]. Dolomite is a form of Calcium Magnesium Carbonate ($CaMg(CO_3)_2$) with a strong peak at 1099 cm^{-1} and minor peaks at 724, 1321, 1442, 1596, and 1760 cm^{-1}. Dolomite is geologically formed at high temperatures in the earth's crust. In the human body, it has previously been found in urinary stones, and it is a diagenetic phase transition from calcite[26,27].

Anatase and rutile are titanium dioxide (TiO_2) polymorphs, with weak positive birefringence (Δn = 0.073). Due to their small (<1 μm size), they could not previously be identified with CPLM. Anatase is identified by Raman with characteristic peaks at 394, 516, and 638 cm^{-1} and rutile with characteristic peaks at 446 and 608 cm^{-1}.

Titanium dioxide is a known component of many products, including paints and items used for personal and medical care, and the release of titanium nanoparticles due to the wear and tear of titanium implants has been suggested[28]. From in vitro studies, it is known that titanium dioxide crystals like anatase and rutile have inflammatory properties, like MSU and CPP. Vallès et al. demonstrated that cultured THP-1 cells subjected to rutile particles released cytokines TNF-α, IL-6, and IL-1β[29].

Thenardite is a form of sodium sulfate (Na_2SO_4) and has a strong peak at 992 cm^{-1}, and some minor peaks at 450, 466, 620, 632, 648, 1101, 1131, and 1153 cm^{-1}. Sodium sulfate is occasionally used as a laxative and can be used as an additive for food. The physiological process behind presentation in SF and whether it can act as an inflammatory agent is unknown.

We also measured spectra of lipid spherules, which are known as Maltese Cross birefringent objects (Fig 1). The Malteser Cross lipid spherules showed bands indicating the presence of fatty acids at 1266, 1304, and 2852 cm^{-1}, unsaturated fatty acids at 1656 and 3012 cm^{-1}, cholesterol at 702, 1442, and 1669 cm^{-1}, and lipids at 1752, 2852, and 2890 cm^{-1}. A large blob with similar spectral properties was also found. While being similar in material, this lacks birefringence, and their presence has not been previously noticed. Near the lipid spherules, we also

found some deposited carotenoids. The carotenoid spectrum can be identified from the peaks at 1002, 1160, and 1522 cm^{-1}.

While the presence of these lipid spherules is long known, their pathologic relevance remains unknown. Carotenoids are vitamin A lipophilic precursor molecules, thus their presence in the vicinity of these spherules may be related.

3.1 Crystal identification in patient samples

We analyzed 28 synovial fluid samples. These patients all had swollen joints and were suspected of crystalline arthritis. In each sample, we analyzed 5-10 crystals. The results of this analysis are shown in table 1. Most of the samples (19/28) contained at least one of the previously known pathological synovial crystals. MSU crystals were found in 13 samples, CPP was found in seven samples. We detected hydroxyapatite in three samples and one sample contained calcium oxalate monohydrate crystals. We did not find the presence of deposited cholesterol and deposited pharmaceuticals, which are known to be present in synovial fluids after treatment[30-32]. We did however find several other crystals.

Calcium carbonate crystals (calcite, aragonite, and with magnesium, dolomite) were the most prominent of the novel crystals and were found in 11 individual samples. Thenardite was found in 5 samples and titanium dioxide crystals (anatase, rutile) were found in 4 samples. Titanium dioxide is not a byproduct of physiological processes, and the presence of these particles must be from foreign origin. While patient 28 had a bilateral titanium alloy hip implant five years before his swollen ankle[33], we could not establish such relationships with samples 19, 21, and 27.

The lipid spherules were found in two cases. In both cases, the arthritis turned out to be a soft-tissue tumor, patient 20 had a myxofibrosarcoma and patient 21 had a lipoma arborescence. Finding these particles in the presence of these rare types of tumors is interesting and a possible relationship may be investigated further.

Looking at these results, we can diagnose 13 instances of gout and 7 instances of CPPD. A combination of multiple crystals, referred to as mixed crystal disease[34], was found in 13 patients. Mixed crystal disease is known as a very rare condition and these results demonstrate that this might not be the case. It is interesting that co-findings of novel crystals were more frequent in samples containing CPP (4/7) than MSU (4/13). The relationship between the presence of these additional crystals and the severity of the disease is still unknown; whether their presence is a confounder in inflammation or joint erosion should be established in future research.

There is more research required to establish possible pathologic roles of the novel discovered crystals and the combinations of crystals. The presence of some of the crystals is not incidental, which means that they were previously missed with polarized light microscopy. This shows the relevance of objective, specific microscopic techniques like HRI. With the current setup, the measurement of a single crystal took seven minutes. Further analysis of data took several additional minutes. Therefore, we were able to analyze and detect five to ten crystals per patient and we are not that certain on the significance of our results on the clinical diagnosis. In gout and CPP associated arthritis, crystal counts range from several to hundreds of crystals in a single sample. Previous methods which applied Raman for the identification of synovial crystals showed to be more sensitive for diagnostic purposes but also missed a significant number of crystal types that we did detect. Furthermore, HRI can detect very small crystals, with a size of 400 nm. If HRI would be applied for diagnostic purposes, there are some technological gaps

to overcome. Full analysis of a single sample with the current method took up to 1.5 hours, which is more than the conventional method. With a more automated and faster method, HRI might offer an accurate and objective platform for crystal identification, especially when combined with a Raman spectral database. In future projects, we will work on the implementation of an automated HRI method in clinical care.

4. Conclusion

In this proof-of-concept study, we demonstrated the potential added value of HRI to synovial crystal research. We identified known synovial crystals MSU, CPP, HA, and COM but HRI also enabled us to identify so far unknown crystals and combinations of crystals from synovial fluid. While the clinical value of these novel crystals is yet unknown, it demonstrates that there is much to be learned about intra-articular and synovial crystals. Possibilities are that these results lead to the discovery of novel crystal-based diseases. Proceedings are needed on Raman-based crystal identification and a database of Raman spectra from synovial crystals. The prospect is that this will offer more understanding of the pathologic pathways behind crystal-related disease and allow us to provide more accurate diagnoses and disease monitoring.

AUTHOR INFORMATION

Corresponding Author

* Tom Niessink, t.niessink@utwente.nl, Drienerlolaan 5, 7500AE, Enschede, the Netherlands

Author Contributions

TN: Drafted manuscript, analyzed data. **BJ**: Measured samples, collected data. **CK**: Measured samples, collected data. **AL**: Raman setup **MJ**: Set up study, supplied images, supplied patient samples, reviewed manuscript. **TLJ**: Set up study, supplied patient samples, reviewed manuscript. **CO**: Set up study, analyzed data, reviewed manuscript.

Notes

Declarations of interest:

CO: CEO of Hybriscan Technologies BV, Nijkerk, the Netherlands. Hybriscan produces multiple types of microscopic imaging modalities, including a Raman integrated polarized light microscope.

MJ, TLJ: Owners of Human Crystal Research BV, Venlo, the Netherlands. HCR BV is specialized in the analysis of synovial crystals and will establish a database of Raman spectra from SF crystals.

ACKNOWLEDGMENTS

The collaboration project is co-funded by the PPP Allowance made available by Health-Holland, Top Sector Life Sciences & Health, to Stichting ReumaNederland to stimulate public-private partnerships.

REFERENCES

(1) Mulay SR, Anders H-J *New England Journal of Medicine* **2016**, *374*, 2465.

(2) Zhang W, Doherty M, Bardin T, Barskova V, Guerne PA, Jansen TL, Leeb BF, Perez-Ruiz F, Pimentao J, Punzi L, Richette P, Sivera F, Uhlig T, Watt I, Pascual E *Ann Rheum Dis* **2011**, *70*, 563.

(3) Richette P, Doherty M, Pascual E, Barskova V, Becce F, Castaneda J, Coyfish M, Guillo S, Jansen T, Janssens H, Lioté F, Mallen CD, Nuki G, Perez-Ruiz F, Pimentao J, Punzi L, Pywell A, So AK, Tausche A-K, Uhlig T, Zavada J, Zhang W, Tubach F, Bardin T *Annals of the Rheumatic Diseases* **2020**, *79*, 31.

(4) Richette P, Doherty M, Pascual E, Barskova V, Becce F, Castañeda-Sanabria J, Coyfish M, Guillo S, Jansen TL, Janssens H, Lioté F, Mallen C, Nuki G, Perez-Ruiz F, Pimentao J, Punzi L, Pywell T, So A, Tausche AK, Uhlig T, Zavada J, Zhang W, Tubach F, Bardin T *Annals of the Rheumatic Diseases* **2017**, *76*, 29.

(5) Zhang W, Doherty M, Pascual E, Barskova V, Guerne PA, Jansen T, Leeb B, Perez-Ruiz F, Pimentao J, Punzi L, Richette P, Sivera F, Uhlig T, Watt I, Bardin T *Annals of the rheumatic diseases* **2011**, *70*, 571.

(6) Schumacher HR, Jr., Sieck MS, Rothfuss S, Clayburne GM, Baumgarten DF, Mochan BS, Kant JA *Arthritis Rheum* **1986**, *29*, 770.

(7) von Essen R, Hölttä AMH, Pikkarainen R *Annals of the Rheumatic Diseases* **1998**, *57*, 107.

(8) McGill NW, York HF *Aust N Z J Med* **1991**, *21*, 710.

(9) Gordon C, Swan A, Dieppe P *Ann Rheum Dis* **1989**, *48*, 737.

(10) Lumbreras B, Pascual E, Frasquet J, González-Salinas J, Rodríguez E, Hernández-Aguado I *Ann Rheum Dis* **2005**, *64*, 612.

(11) Berendsen D, Neogi T, Taylor WJ, Dalbeth N, Jansen TL *Clin Rheumatol* **2017**, *36*, 641.

(12) Hosu CD, Moisoiu V, Stefancu A, Antonescu E, Leopold LF, Leopold N, Fodor D *Lasers in Medical Science* **2019**, *34*, 827.

(13) McGill N, Dieppe PA, Bowden M, Gardiner DJ, Hall M *The Lancet* **1991**, *337*, 77.

(14) Abhishek A, Curran DJ, Bilwani F, Jones AC, Towler MR, Doherty M *Rheumatology* **2015**, *55*, 379.

(15) Curran DJ, Rubin L, Towler MR *Clin Med Insights Arthritis Musculoskelet Disord* **2015**, *8*, 55.

(16) Li B, Singer NG, Yeni YN, Haggins DG, Barnboym E, Oravec D, Lewis S, Akkus O *Arthritis & rheumatology (Hoboken, N.J.)* **2016**, *68*, 1751.

(17) Cheng X, Haggins DG, York RH, Yeni YN, Akkus O *Applied Spectroscopy* **2009**, *63*, 381.

(18) Li B, Yang S, Akkus O *2013 Conference on Lasers and Electro-Optics, CLEO 2013* **2013**.

(19) Zhang B, Xu H, Chen J, Zhu X, Xue Y, Yang Y, Ao J, Hua Y, Ji M *Theranostics* **2021**, *11*, 3074.

(20) Drozdovskiy I, Ligeza G, Jahoda P, Franke M, Lennert P, Vodnik P, Payler SJ, Kaliwoda M, Pozzobon R, Massironi M, Turchi L, Bessone L, Sauro F *Data Brief* **2020**, *31*, 105985.

(21) Lafuente B, Downs RT, Yang H, Stone N In *Highlights in Mineralogical Crystallography*; Thomas A, Rosa Micaela D, Eds.; De Gruyter (O): 2015, p 1.

(22) Lorenz EC, Michet CJ, Milliner DS, Lieske JC *Curr Rheumatol Rep* **2013**, *15*, 340.

(23) Hongsmatip P, Cheng KY, Kim C, Lawrence DA, Rivera R, Smitaman E *European Journal of Radiology* **2019**, *120*, 108653.

(24) Yu JK, Pan H, Huang SM, Huang NL, Yao CC, Hsiao KM, Wu CW *Asian J Surg* **2013**, *36*, 26.

(25) Tabei Y, Sugino S, Eguchi K, Tajika M, Abe H, Nakajima Y, Horie M *Biochem Biophys Res Commun* **2017**, *490*, 499.

(26) Keshavarzi B, Yavar Ashayeri N, Moore F, Irani D, Asadi S, Zarasvandi A, Salari M *Minerals* **2016**, *6*, 131.

(27) Sivaguru M, Saw JJ, Wilson EM, Lieske JC, Krambeck AE, Williams JC, Romero MF, Fouke KW, Curtis MW, Kear-Scott JL, Chia N, Fouke BW *Nature Reviews Urology* **2021**, *18*, 404.

(28) Yao JJ, Lewallen EA, Trousdale WH, Xu W, Thaler R, Salib CG, Reina N, Abdel MP, Lewallen DG, van Wijnen AJ *BioResearch open access* **2017**, *6*, 94.

(29) Vallés G, González-Melendi P, González-Carrasco JL, Saldaña L, Sánchez-Sabaté E, Munuera L, Vilaboa N *Biomaterials* **2006**, *27*, 5199.

(30) Dey B, Khonglah Y, Raphael V, Dange P *J Family Med Prim Care* **2020**, *9*, 4428.

(31) Ettlinger RE, Hunder GG *Mayo Clin Proc* **1979**, *54*, 366.

(32) Young P, Homlar KC *Am J Orthop (Belle Mead NJ)* **2016**, *45*, E108.

(33) Niessink T, Ringoot J, Janssen M, Otto C, Jansen T *Arthritis & Rheumatology*, *n/a*.

(34) Pascual E, Sivera F, Andres M *The Journal of Rheumatology* **2020**, *47*, 1158.

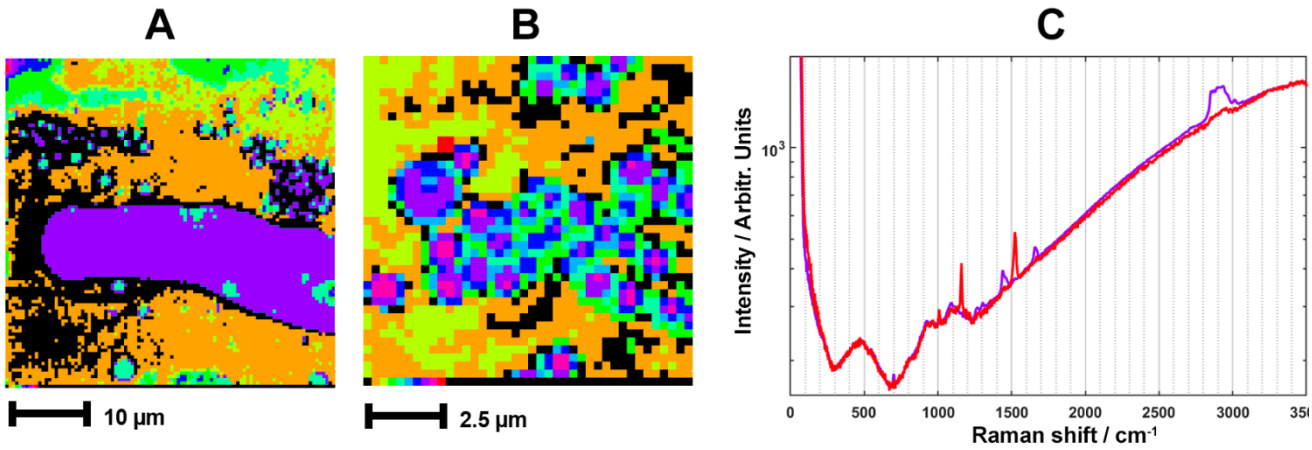

Figure 1: Raman cluster analysis of a sample containing lipid spherules, also referred to as 'Maltese Cross Birefringent Objects'. The purple spectrum refers to the lipid spherules, the red spectrum in C shows a small deposition of a carotenoid compound, marked with the white circle in the left image. Visible is both the spherules (B) as the large fatty acid blob (A), which has similar spectral properties as the spherules. The large fatty acid blob was not earlier observed with CPLM. Dimensions of A are 100x100 pixels in 40x40 µm, dimensions of B are 40x40 pixels in 10x10 µm.

Patient	MSU	triclinic CPP	Hydroxyapatite	COM	Calcite	Aragonite	Anatase	Rutile	Thenardite	Dolomite	Maltese Crosses	Carotenoid	Defined as
1 to 9	•												**Gout**
10	•				•								
11	•								•				
12	•		•										
13	•	•	•										**Mixed**
14 to 16		•											**CPPD**
17		•							•	•			
18		•				•							
19		•		•	•			•					
20											•	•	**Unknown**
21							•				•		
22			•		•								
23					•								
24					•								
25									•				
26					•				•				
27					•		•					•	
28					•		•						

Table 1: Distribution of found crystals in patients with suspected gout or CPPD. MSU = monosodium urate, CPP = calcium pyrophosphate, COM = calcium oxalate monohydrate. A dot (•) represents the presence of one or more crystals of this type in this sample. Note that patients 1-9 and 14-16 are summarized in one table entry. According to these results, patients 1-12 can be diagnosed with gout and patients 14-19 can be diagnosed with CPPD. Patient 13 presents crystals related to both gout and CPPD. Patients 20-28 remain undiagnosed.

Raman hyperspectral imaging detects novel and combinations of crystals in synovial fluids of patients with a swollen joint

Authors: Tom Niessink (MSc.)[1,2*], Charline Kuipers (MSc.)[1], Brighton de Jong (BSc.)[1], Aufried Lenferink (Bsc.)[1], Matthijs Janssen (MD., PhD.)[2], Tim L Jansen (MD., PhD.)[1,2], and Cees Otto (PhD.)[1]

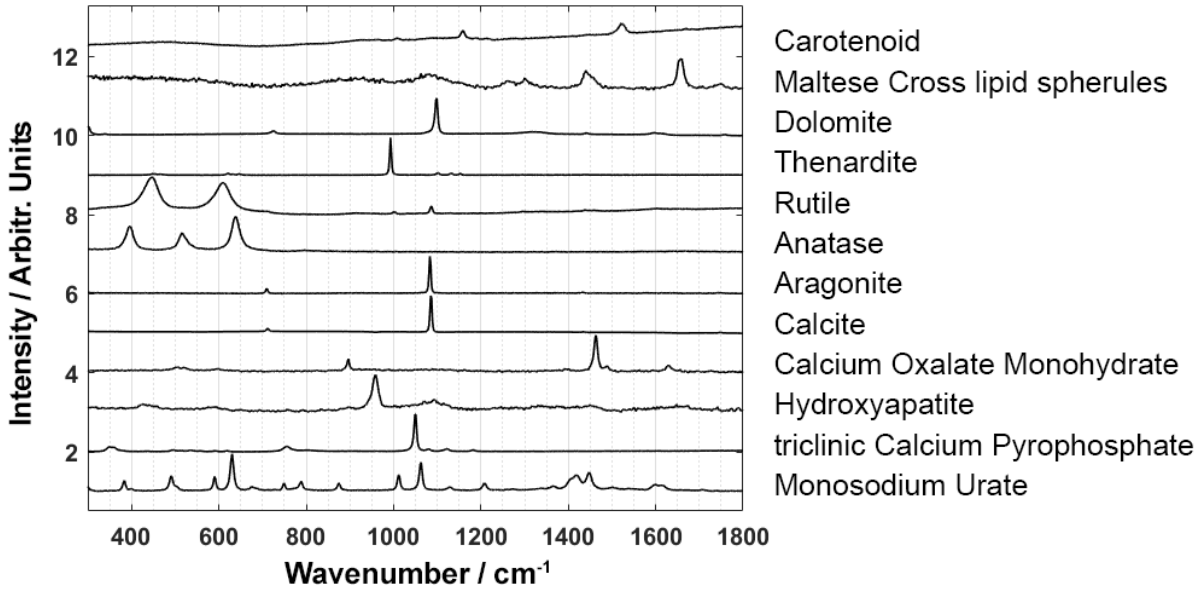

Graphical table of contents: Measured Raman spectra of crystals found in synovial fluids of patients with suspected gout or calcium pyrophosphate deposition disease.